ChemComm

Accepted Manuscript

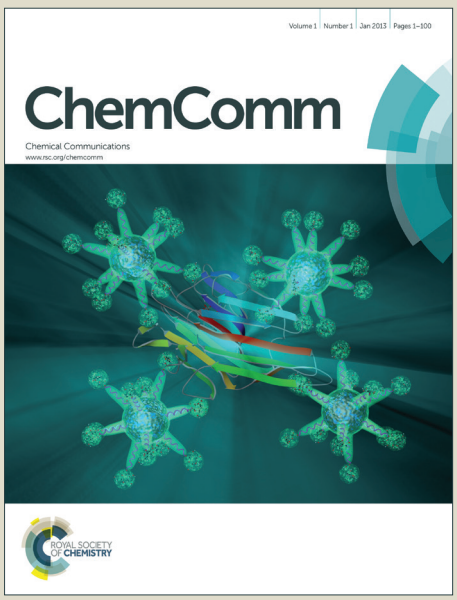

ROYAL SOCIETY OF CHEMISTRY

www.rsc.org/chemcomm

Journal Name

RSCPublishing

COMMUNICATION

Two Solvent Grinding Sonication Method for the Synthesis of Two-dimensional Tungsten Disulphide Flakes

.Cite this: DOI: 10.1039/x0xx00000x

Received ooth January 2012,
Accepted ooth January 2012

DOI: 10.1039/x0xx00000x

www.rsc.org/

Benjamin J. Carey[a,b], Torben Daeneke[a], Emily P. Nguyen[a,b], Yichao Wang[a], Jian Z. Ou[a], Serge Zhuiykov[b] and Kourosh Kalantar-zadeh[a]

Two-dimensional tungsten disulphide flakes are developed via a two solvent grinding assisted liquid phase exfoliation method. Our investigations show the distinct advantages of this approach that include reduced residues of the solvent used, high yield and creating relatively thin flakes suitable for electronic, optical, catalytic and energy storage applications.

Two dimensional transition metal dichalcogonides (2D TMDs) feature many exotic and unique electronic, optical, chemical and mechanical properties. Such properties make them favourable for potential applications in electronic and optical devices, sensors, catalysis as well as energy storage and conversion.[1-8]

2D TMDs can be produced using several different methodologies such as mechanical and liquid phase exfoliation techniques from their bulk stratified crystals as well as directly via chemical vapour deposition. [8] Liquid phase exfoliation is used in the high yield, scalable production of 2D TMDs, however the relevant outcomes from this process are highly sensitive to the procedures' parameters.[2, 7-12] A vast host of liquid phase exfoliation techniques have been introduced. Such as Intercalation [10, 13], laser ablation [11, 12] and ultrasound exfoliation [2, 7], with grinding assisted ultrasonic exfoliation being one of the most attractive methods due to its high yield, while avoiding the use of hazardous reagents such as butyllithium.[13]

During ultrasonic exfoliation the solvent selection plays an important part, since physical properties such as boiling point [14], surface tension and energy, [2, 3] along with solubility parameters [15] affect the process and hence the resulting 2D flakes. There are still many challenges and unknowns when utilizing sonication exfoliation methodologies and further work is necessary in order to understand the process and improve the quality of the resulting 2D TMD flakes. One particularly promising 2D TMDs is tungsten disulphide (WS_2).[5, 16]. In comparison to most of the other 2D TMDs, 2D WS_2 offers better chemical stabilities, while featuring certain favourable electronic characteristics.[3, 17] There are now well-established methods for obtaining durable p and n type semiconducting 2D WS_2 that makes it amongst the most suitable 2D TMDs for developing future IC chips, optical components, catalysts as well as analytical and bio systems.[1] Producing high quality, large surface area and relatively pure 2D WS_2 flakes utilizing a scalable method is still a challenge and further research is necessary to investigate the suitability of liquid phase exfoliation techniques for this purpose.

In this study the effects of solvent selection were experimentally assessed for grinding assisted ultrasound liquid phase exfoliation by evaluating a methodology that comprises of using different solvents for the grinding and sonication processes. A popular high yield solvent, N-methyl-2-pyrrolidone (NMP), which has been recommended in several studies was employed as a high yield reference. [2, 9, 18] Even though high yields are obtained when using NMP, solvent residues were found to be difficult to remove due to its relatively high boiling point (202°C) and surface tension (40.79 mJ m^{-2} at 20°C). [19] Residual NMP can often be found on the resulting 2D materials, even when post processing methods aiming at the solvent removal are used.[15] The inherent instability of NMP is further complicating its removal since NMP is known to polymerize at elevated temperatures which occur during sonication and solvent evaporation.[20] Solvent residues and degradation products are detrimental to many applications of 2D TMDs such as catalysis and sensing which require a pristine surface. Furthermore the electronic properties of the resulting flakes are likely to be altered by organic residues. In order to find alternative solutions, able to overcome the limitations of exfoliation in NMP, acetonitrile (ACN) and a 50/50 ethanol/water mixture were initially investigated as solvents. These good process solvents are chosen as they offer moderate boiling points and their residues can be readily removed.

For the liquid exfoliation process using NMP, ACN and ethanol/water solvents, the WS_2 bulk powder was separately ground in each solvent and then sonicated in the same solvent as grinding (details of the exfoliation methodology are presented in supplementary information). Figure 1a shows an image of the resulting 2D WS_2 suspensions. While the NMP solution resulted in high yield (Figure 1a i), as expected, the observed yields for the ACN and ethanol/water solutions were low, evident through the low coloration of the suspensions (Figure 1a ii and iii).

A fourth suspension was investigated with a modified process step to possibly increase the yield. In this case, the grinding and sonication solvents were chosen to be different. We refer to this process as the 'two solvent method' which has previously been shown effective for obtaining 2D MoS_2. [21] ACN was used during the grinding step and the 50/50 ethanol/water mixture during the sonication step (after the grinding solvent was evaporated). In this case, a dramatic increase of the yield was evident due to the more intense coloration of the fourth suspension (Figure 1a iv). The reverse methodology (grinding with ethanol/water and sonicated in ACN) was also investigated leading to negligible exfoliation yield (as shown in the supplementary information). Our following characterizations will demonstrate why the choice of ACN as the grinding solvent and the ethanol/water mix as the sonication solvent provided this improvement.

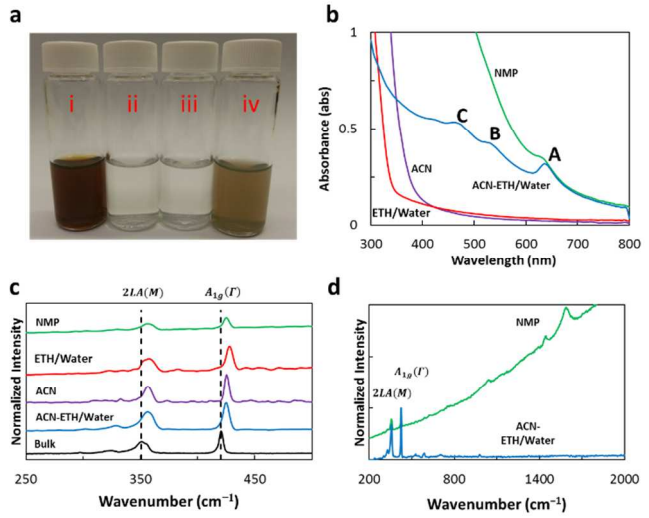

Figure 1: (a) Image of the 2D WS_2 flakes suspensions prepared with NMP (i), ACN (ii), ethanol/water (iii) and the two solvent method (iv). (b) UV-Vis absorption spectra of the 2D WS_2 suspensions with the A, B and C excitons marked. Note both the NMP and the two solvent (ACN-ETH/Water) solutions were diluted 1 part in 4 from the optical image for the UV-Vis measurement. (b) & (c) Raman spectra of 2D WS_2 flakes. Spectra have been normalized to the $A_{1g}(\Gamma)$ phonon peak. (c) The position of the $2LA(M)$ and $A_{1g}(\Gamma)$ phonons (from bulk WS_2) have been marked and spectra have been vertically offset for clarity.

The UV-vis spectra of the suspensions can be observed in Figure 1b. From this the concentration of the solutions were calculated to be 0.14 mg/ml, 1.46 µg/ml, 0.82 µg/ml and 0.1 mg/ml for NMP, ACN, ethanol/water and the two solvent method respectively indicating the superiority of the two solvent method over both ACN and ethanol/water (details are shown in the supplementary information). The peaks of 635, 530 and 475 nm (A, B and C respectively) are clearly seen for the two solvent processed suspension which are known to be due to the excitonic absorption of 2D WS_2 suspensions, emphasizing the existence of a direct bandgap associated with a small number of layers. [1] Excitonic peak A is also observed for flakes exfoliated in NMP. The excitonic peaks B and C are however not observed in this case. The disappearance and reduction of the intensity of the excitonic peaks have been suggested to be associated with the decrease in the lateral dimensions of the flakes when NMP is used. [22] In our case, however, it seems that the interaction between NMP and/or the NMP decomposition products and the WS_2 surface are likely to alter the electronic structure of the semiconducting flakes leading to more intense absorption of high energy photons obscuring excitonic effects.

The phonon peaks $2LA(M)$, $E^1_{2g}(\Gamma)$ and $A_{1g}(\Gamma)$ in the Raman spectrum of the non-exfoliated (bulk) powder are observed at 350.6, 356 and 420.4 cm^{-1} shift to higher wave numbers (~353, ~358 and ~425 cm^{-1}, respectively) after exfoliation (Figure 1b and Table S1). The shift of the Raman peaks and the increase of the $E^1_{2g}(\Gamma)$ phonon (table s2) is characteristic for the formation of thin WS_2 flakes. [23]

Raman spectra for NMP exfoliated flakes (Figure 1d) showed strong fluorescence induced by the excitation laser evident in the intense background signal and the deviation from a flat baseline. This behaviour is not observed in the two solvent method exfoliated flakes, highlighting differences in the electronic structure of the resulting material even after the solvent drying stage. The phonon peaks are quenched for NMP exfoliated flakes and a characteristic NMP Raman signal is observed featuring peaks at 1450 and 1600 cm^{-1} highlighting that a significant amount of the NMP solvent residues and decomposition products remained on the 2D WS_2 surface, despite of drying the flakes at 70°C for 4 hours. These residues are likely to interfere with 2D WS_2 applications that require pristine surfaces such as catalysis, gas/bio sensing and certain electronic devices. The NMP effect also reduces the accuracy of the number of layer assessment using Raman spectroscopy. However, samples prepared following the two solvent exfoliation method showed no signs of residues in the Raman spectrum confirming the two solvent approach as a superior exfoliation technique.

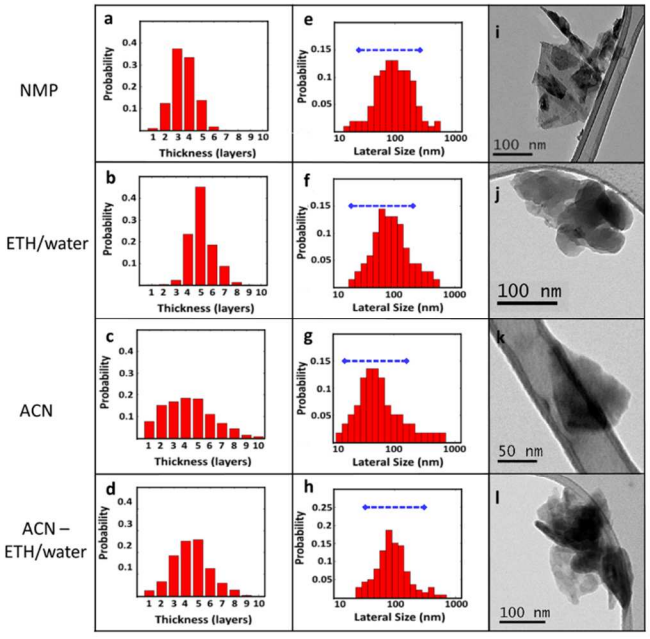

Figure 2: (a-d) Statistical distribution of WS_2 flake thickness analysed from AFM imagining. (e-h) statistical distribution of lateral dimensions analysed from TEM imagining. The blue overlay is an approximation of flake size based on DLS. † (i-l) TEM images of the WS_2 flakes synthesized with different solvent methods.

The thickness distribution and polydispersity of the exfoliated WS_2 flakes was assessed by atomic force microscopy (AFM), transmission

electron microscopy (TEM) and dynamic light scattering (DLS) techniques.

The physical dimensions are summarized in Figure 2. Here the effect that solvent selection has upon the physical characteristics of the produced flakes becomes fairly evident. NMP produces many thin flakes (≤4 layers) with relatively large surface areas (median = 98 nm) while ethanol/water produced flakes of similar lateral polydispersion (median = 87 nm), however with a tendency towards thicker, less two-dimensional flakes (≥5 layers). ACN produced a large fraction of single and two layer flakes with a large horizontal polydispersity and overall reduced the lateral sizing (median = 51 nm). The two solvent method produced flakes with size characteristics of 90 nm median lateral dimension with many ≤4 layer flakes, suggesting a combination of the flake properties between the ethanol/water and ACN systems which was overall effectively closer to that of the archetypal NMP based exfoliation.

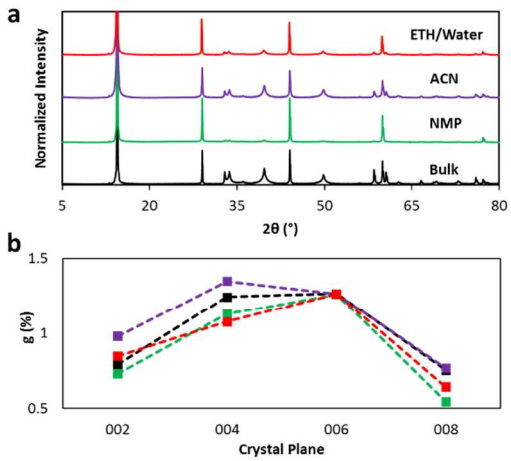

Figure 3: (a) XRD of bulk WS_2 powder and WS_2 powder after grinding (pre exfoliation). The results have been normalized to the 002 peak, offset vertically and the 002 peak has been clipped for clarity. (b) Paracrystallinity factor (g) of the vertical crystal planes for bulk WS_2 powder (black) and WS_2 powder after grinding in NMP (green), ACN (purple) and ethanol/water (50/50, red)

To elucidate the origin of the yield variation and the yield increase following the implementation of the two solvent method, X-ray diffraction (XRD) patterns of the ground (non-exfoliated) and dried powders were taken prior to sonication. Figure 3a) shows several solvent dependent variations in the XRD pattern indicating changes in crystallinity after grinding the bulk WS_2. The 002, 004, 006 and 008 peaks (at 14.5°, 29°, 44°, and 60°, respectively) are of particular interest since these peaks are arising from the symmetry of the vertical crystal planes (layer to layer crystallinity). The paracrystallinity factor (PF) allows to assess the crystallinity of a sample (Figure 3b). The PF was calculated using the cold-work distortion method, [24] which has been previously used for similar materials (see supplementary information for details).[25] Increased PF values indicate lower short term order. A breakdown of vertical order as indicated by the PF is just seen for the ACN ground samples. This reduction in the short term order of the 002 plane can also be indicated by the broadening of the 002 peak (the calculated full-width half-maximum (FWHM) is presented in Table S2). The FWHM of the 002 peak is most effectively increased when grinding with ACN. NMP and ethanol/water did however also broaden the 002 peak indicating some reduction in the vertical order. The XRD patterns are providing an explanation for the increased exfoliation yield when using the two solvent method. The vertical order is most effectively broken down by grinding in ACN. Zhou et al. investigated the suitability of different ethanol/water mixtures for the sonication step during the WS_2 exfoliation and found a correlation between the exfoliation yield and the Hansen solubility parameters (HSP) of the solvent.[14] A HSP-distance of 13.1 is calculated for the ethanol/water mixture while ACN leads to a calculated HSP-distance of 19.2 (see supplementary information for details). A lower HSP-distance leads to a higher expected solubility. The observed difference in HSP-distance between the solvent systems was comparatively large. These results demonstrate that the required solvent parameters during grinding and sonication may be very different and potentially unrelated.

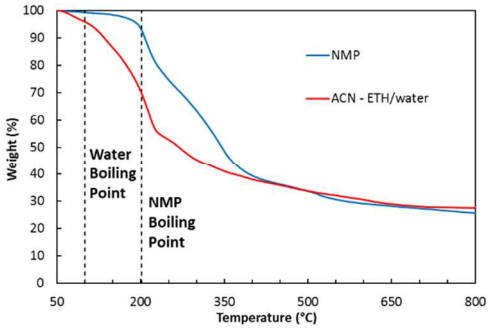

Figure 4: TGA of the dried 2D WS_2 flakes prepared with both only NMP and ACN-ethanol/water two solvent methods tested in nitrogen gas. The boiling points of both NMP and water are marked (202°C and 100°C at standard pressure)

Thermal gravimetric analysis (TGA, Figure 4) was employed to assess the extent of NMP (for the single solvent process using NMP) as well as ACN and ethanol (for the two solvent method) residues on the dried 2D WS_2 flakes. It can be seen that due to the large surface area of the 2D WS_2 flakes over 60% w/w of the product constitutes surface bound solvent molecules and solvent decomposition products, even after drying in vacuum at elevated temperatures (100 hr at 70°C). High temperatures of over 200°C were necessary to start the NMP desorption process. Flakes prepared following the two solvent method show weight loss at significantly lower temperatures indicating that predominantly water and potentially ethanol residue were present on the WS_2 surface which were removed with comparative ease. This exceedingly high absorbed solvent to solid ratio could potentially open up many doorways to applications such as dehumidification, solvent absorption and gas/bio sensing. This property of 2D WS_2 can be rationalized considering the large aspect ratio of the flakes and their surface polarity.

Conclusions

A two solvent exfoliation method was developed and investigated for the synthesis of relatively small thickness 2D WS_2 flakes at high yields. For comparison the resulted 2D flake suspension was assessed in reference to those obtained using the single solvent method. It was demonstrated that the choice of a separate grinding solvent prior to the sonication in liquid phase exfoliation played a major role in the

determination of the process that has been largely overlooked to date. The two solvent method based on grinding with ACN and sonication in ethanol/water mix resulted in much higher yield in comparison to single solution grinding sonication method using ACN and ethanol/water solutions alone.

AFM, TEM and DLS characterizations revealed that the lateral size and thickness of the exfoliated flakes depend highly on the chosen solvent during both the grinding and sonication steps. They showed that the two solvent method generated flakes comparable to those of NMP solution in terms of lateral size and thickness. Raman and UV-Vis spectroscopy provided strong evidence that NMP residues remained on the surface of the exfoliated flakes, interfering with many of the desired properties of 2D WS_2. However, such adverse effects of the residues seem to be reduced using the two solvent method.

XRD was performed on the WS_2 powder after the grinding step in order to understand the origin of the yield variation. The XRD results confirmed that ACN does reduce interlayer crystallinity more efficiently than the other solvents.

A >60% w/w solvent content was later confirmed with TGA for both NMP and two solvent exfoliated flakes. The NMP contamination required however a higher temperature for its removal.

This work helps to increase the understanding of the importance of the grinding step during the grinding assisted ultrasound exfoliation of 2D materials which has been poorly understood to date. It also suggests that choice of two separate solvents for grinding and sonication processes are highly beneficial. Future work should carefully evaluate, if surface bound molecules on the 2D WS_2 surface can interfere with or even be utilized for the intended applications. Additionally, further research of different two solvent method combinations may lead to increased exfoliation yields and larger lateral dimensions of the flakes with clean surfaces.

Notes and references

[a] School of Electrical and Computer Engineering, RMIT University, Melbourne, Victoria, Australia

[b] Division of Materials Science and Engineering, CSIRO, Highett, Victoria, Australia

E-mails: kourosh.kalantar@rmit.edu.au & torben.daeneke@rmit.edu.au

† Approximation of 2D flake lateral dimensions from DLS results taken from Lotya *et al.* [26]

Electronic Supplementary Information (ESI) available: [additional information on experimental methods, information on reverse two solvent method experiment, tabularized Raman and XRD data, additional sample AFM data including conductive AFM, HRTEM data as well as details of the HSP, concentration and PF calculations can be found in the supporting information]. See DOI: 10.1039/c000000x/

Acknowledgements

The authors acknowledge the facilities, and the scientific and technical assistance, of the Australian Microscopy and Microanalysis Research Facility at RMIT University and of the Commonwealth Scientific and Industrial Research Organisation (CSIRO), Highett, Victoria, Australia. We also acknowledge the fund from Australian Research Council discovery grant (DP140100170).

1. Q. H. Wang, K. Kalantar-Zadeh, A. Kis, J. N. Coleman and M. S. Strano, *Nat Nano*, 2012, **7**, 699-712.
2. J. N. Coleman, M. Lotya, A. O'Neill, S. D. Bergin, P. J. King, U. Khan, K. Young, A. Gaucher, S. De, R. J. Smith, I. V. Shvets, S. K. Arora, G. Stanton, H.-Y. Kim, K. Lee, G. T. Kim, G. S. Duesberg, T. Hallam, J. J. Boland, J. J. Wang, J. F. Donegan, J. C. Grunlan, G. Moriarty, A. Shmeliov, R. J. Nicholls, J. M. Perkins, E. M. Grieveson, K. Theuwissen, D. W. McComb, P. D. Nellist and V. Nicolosi, *Science*, 2011, **331**, 568-571.
3. Q. Tang and Z. Zhou, *Progress in Materials Science*, 2013, **58**, 1244-1315.
4. A. B. Kaul, *Journal of Materials Research*, 2014, **29**, 348-361.
5. M. Chhowalla, H. S. Shin, G. Eda, L.-J. Li, K. P. Loh and H. Zhang, *Nature Chemistry*, 2013, **5**, 263-275.
6. Y. Wang, C. Zhou, W. Wang and Y. Zhao, *Industrial & Engineering Chemistry Research*, 2013, **52**, 4379-4382.
7. V. Stengl, J. Henych, M. Slusna and P. Ecorchard, *Nanoscale Research Letters*, 2014, **9**, 167.
8. S. Das, M. Kim, J.-w. Lee and W. Choi, *Critical Reviews in Solid State and Materials Sciences*, 2014, **39**, 231-252.
9. J. N. Coleman, *Accounts of Chemical Research*, 2013, **46**, 14-22.
10. V. Nicolosi, M. Chhowalla, M. G. Kanatzidis, M. S. Strano and J. N. Coleman, *Science*, 2013, **340**, 6139.
11. P. Kumar, *Rsc Advances*, 2013, **3**, 11987-12002.
12. H. S. S. R. Matte, U. Maitra, P. Kumar, B. G. Rao, K. Pramoda and C. N. R. Rao, *Zeitschrift Fur Anorganische Und Allgemeine Chemie*, 2012, **638**, 2617-2624.
13. G. Eda, H. Yamaguchi, D. Voiry, T. Fujita, M. Chen and M. Chhowalla, *Nano Letters*, 2011, **11**, 5111-5116.
14. K.-G. Zhou, N.-N. Mao, H.-X. Wang, Y. Peng and H.-L. Zhang, *Angewandte Chemie-International Edition*, 2011, **50**, 10839-10842.
15. U. Halim, C. R. Zheng, Y. Chen, Z. Lin, S. Jiang, R. Cheng, Y. Huang and X. Duan, *Nat. Commun.*, 2013, **4**, 2213.
16. Y. Chen, J. Xi, D. O. Dumcenco, Z. Liu, K. Suenaga, D. Wang, Z. Shuai, Y.-S. Huang and L. Xie, *Acs Nano*, 2013, **7**, 4610-4616.
17. Z. Jin, X. Li, J. T. Mullen and K. W. Kim, *Physical Review B*, 2014, **90**, 045422.
18. A. O'Neill, U. Khan and J. N. Coleman, *Chemistry of Materials*, 2012, **24**, 2414-2421.
19. D. R. Lide, *Physical Constants of Organic Compounds*, CRC Press, Boca Raton, FL, 2005.
20. C. Berrueco, P. Alvarez, S. Venditti, T. J. Morgan, A. A. Herod, M. Millan and R. Kandiyoti, *Energy & Fuels*, 2009, **23**, 3008-3015.
21. E. P. Nguyen, B. Carey, T. Daeneke, J. Z. Ou, K. Latham, S. Zhuiykov and K. Kalantar-Zadeh, *Chemistry of Materials*, 2015, **27**, 53-59.
22. C. Backes, R. J. Smith, N. McEvoy, N. C. Berner, D. McCloskey, H. C. Nerl, A. O'Neill, P. J. King, T. Higgins, D. Hanlon, N. Scheuschner, J. Maultzsch, L. Houben, G. S. Duesberg, J. F. Donegan, V. Nicolosi and J. N. Coleman, *Nature Communications*, 2014, **5**, 4576.
23. A. Berkdemir, H. R. Gutierrez, A. R. Botello-Mendez, N. Perea-Lopez, A. L. Elias, C.-I. Chia, B. Wang, V. H. Crespi, F. Lopez-Urias, J.-C. Charlier, H. Terrones and M. Terrones, *Scientific Reports*, 2013, **3**, 1755.
24. B. E. Warren and B. L. Averbach, *Journal of Applied Physics*, 1950, **21**, 595-599.
25. D. Palit, S. K. Srivastava, M. C. Chakravorti and B. K. Samantaray, *Journal of Materials Science Letters*, 1996, **15**, 1636-1637.
26. M. Lotya, A. Rakovich, J. F. Donegan and J. N. Coleman, *Nanotechnology*, 2013, **24**, 265703.